A bright single layer non-doped orange-red light emitting diode using a symmetric starburst material *via* solution process

Sheng Kong, Lixin Xiao,* Yingliang Liu, Zhijian Chen, Bo Qu and Qihuang Gong*

Received (in Victoria, Australia) 8th January 2010, Accepted 30th March 2010
DOI: 10.1039/c0nj00011f

A symmetric starburst orange-red emitter, 2,4,6-tris((*E*)-2-(10-butyl-10*H*-phenothiazin-2-yl)vinyl)-1,3,5-triazine (TP3T) incorporating phenothiazine as the electron donor and triazine as the electron acceptor, was synthesized. It shows high fluorescence quantum yield (0.42 in toluene) because of the existence of strong intramolecular charge transfer between the phenothiazine and the triazine moieties. The smaller dipole moment for the molecule resulted from its symmetric starburst conformation and larger alkyl group substituents induce weaker interaction of molecules, thus fluorescence quenching can be effectively reduced. Owing to its bipolar structure, both hole and electron transport could be facilitated. A single layer non-doped stable orange-red emission with CIE coordinates at (0.59, 0.41) and a low turn-on voltage of 2.5 V and a maximum luminance of 2935 cd m^{-2} was obtained by using TP3T as the single combination layer of charge transporting and emitter *via* solution process.

Introduction

Organic light-emitting diode (OLED) has received great attention since the landmark work by C. W. Tang *et al.*,[1] which is considered to be the next promising generation of flat-panel display technique. Red emission, as one of the primary parts for full color display, has been generally carried out *via* a host-dopant system to avoid severe concentration quenching.[2,3] However, the doping approach makes it complicated to fabricate devices and the emission chrominance usually shift with the bias voltage. Although a few non-doped red emitters have been reported, most of which adopted linear[4,5] or V-shaped[6,7] donor-π-acceptor-π-donor (D-π-A-π-D) systems to prevent dipole–dipole interaction between molecules, however, a multi-layer structure has been generally employed to improve charge balance and efficiency of the device, which does raise the cost of fabrication. Thomas *et al.*[8] reported a series of non-doped red emitters, and obtained maximum luminance of 5083–9878 cd m^{-2} for single layer devices *via* thermal evaporation process. To develop a cost effective way for device fabrication, Li *et al.*[9] reported a single layer non-doped red polymer device *via* solution process. However, only a maximum luminance of 150 cd m^{-2} could be obtained. Therefore, it is crucial to develop highly efficient single layer non-doped red device with solution process.

For this purpose, here we designed a symmetric starburst molecule incorporating phenothiazine as the electron donor and triazine as the electron acceptor. Firstly, to achieve high fluorescence quantum yield for long wavelength emission, donor-π-acceptor (D-π-A) systems with intramolecular charge transfer instead of simply extending π conjugation should be considered, because D-π-A systems have been proved to be important candidates to construct fluorescent material.[10] It should be noted that the intramolecular charge transfer here refers to a partial electron transfer which can be expressed as $D^{\delta+}$–$A^{\delta-}$ for the charge transfer state, with the probability of $0 < \delta < 1$, which induces enhanced fluorescence, without charge separation ($\delta = 1$) which would result in a decrease in fluorescence as described in our previous report.[11] Secondly, to get a stable red emission, a symmetric molecular conformation needs to be designed to minimize the dipole moment of the emitter containing strong intramolecular charge transfer, because the emission chrominance might shift with the applied voltage when a polar emitter is used for red device based on our previous report.[12] In addition, starburst conformation has been reported as an effective resolution to reduce strong intermolecular interaction to suppress fluorescence quenching.[13,14] Therefore, symmetric starburst molecule with donor-π-acceptor (D-π-A) structure seems to be the resolution to induce weaker intermolecular interaction, weaker orientation under the electric field, and stronger intramolecular charge transfer, thus result in suppressed fluorescence quenching, stable color purity and high quantum efficiency. We previously reported a star-shaped material containing a carbazole moiety as the donor and triazine as the acceptor for non-doped red emission *via* solution process.[15] To increase further the intramolecular interaction, we changed the weaker donor of carbazole component into stronger donor of phenothiazine,[16,17] and obtained 2,4,6-tris((*E*)-2-(10-butyl-10*H*-phenothiazin-2-yl)-vinyl)-1,3,5-triazine (TP3T). Owing to the stronger intramolecular charge-transfer, the newly obtained symmetric starburst TP3T exhibits high fluorescence quantum yield (0.42 in toluene), a similar result was reported by Yuan *et al.*[18] The larger alkyl group (from ethyl group in our previous report to butyl group in this work) substitution endow it with more effective suppression of fluorescence quenching in solid state. As a result, single layer non-doped stable orange-red emission with Commission International de l'Eclairage (CIE) coordinates at (0.59, 0.41) and a low turn-on voltage of 2.5 V and a maximum

State Key Laboratory for Mesoscopic Physics and Department of Physics, Peking University, Beijing 100871, China. E-mail: xiao66@pku.edu.cn, qhgong@pku.edu.cn; Fax: +86 10 6275 6567

luminance of 2935 cd m^{-2} was obtained using TP3T as the single combination layer of charge transporting and emitter *via* solution process. In the case of an orange-red single layer device, Liu *et al.*[19] recently achieved a maximum luminance of 947 cd m^{-2} by using a binuclear aluminium complex. However, a host-dopant system was still adopted to avoid severe concentration quenching. It should be noted that TP3T based single layer device reported here is by far the most efficient non-doped single layer orange-red device *via* solution process.

Experimental

General

The ^{1}H NMR and ^{13}C NMR spectra were recorded on a Bruker DPX-400 spectrometer (400 MHz). Elemental analysis was carried out on an Elementar Vario MICRO CUBE (Germany) instrument. Mass spectra were recorded on a Bruker Apex IV FTMS instrument. FT-IR spectra were acquired on a Nicolet Magna IR-750 spectrometer. Photoluminescence (PL) spectra were measured on a Hitachi F-4500 fluorescence spectrophotometer. Ultraviolet-visible (UV-vis) absorption was obtained on an Agilent 8453E UV-vis spectroscopy system. The fluorescent quantum yield was measured in toluene and calculated with dye C152 in ethanol as the standard. The electrochemical properties were measured at a scanning rate of 0.1 V s^{-1} by cyclic voltammetry (CV) on a CHI 660C electrochemistry workstation with a three-electrode configuration. Thermal properties were determined by thermogravimetric analysis (TA Instrument Q50) and differential scanning calorimetry (TA Instrument Q100).

Synthesis

All chemicals were used as received. *N*-Butyl-phenothiazine (compound **1**) and *N*-butyl-3-formyl-phenothiazine (compound **2**) were synthesized according to our previous procedure.[20] 2,4,6-Trimethyl-1,3,5-*s*-triazine was prepared according to the literatures.[21,22] TP3T was prepared according to the synthesis route shown in Scheme 1.

Synthesis of *N*-butyl-phenothiazine (1)

1-Bromobutane (3.84 g, 28 mmol) was added dropwise to a mixture of phenothiazine (5.00 g, 25 mmol) and NaH (1.80 g) in *N*,*N*-dimethylformamide (DMF, 30 mL), and followed by refluxing for 2 h. After cooling down to room temperature, the obtained mixture was poured into distilled water (300 mL), extracted with n-hexane three times (200 mL for each), and dried with anhydrous magnesium sulfate for overnight. *n*-Hexane was evaporated under reduced pressure, and the remaining crude product was purified by silica-gel column chromatography with n-hexane as an eluent. A yellow viscous product was obtained after drying with a yield of 81% (5.19 g).

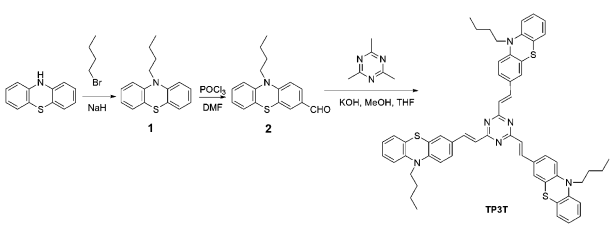

Scheme 1 Synthetic route of TP3T.

Synthesis of *N*-butyl-3-formyl-phenothiazine (2)

Phosphorus oxychloride (20.0 g, 0.13 mmol) was added dropwise to a mixture of DMF (40 mL) and 1,2-dichloroethane (26 mL) and cooled down to 0 °C. Then, **1** (4.0 g, 13 mmol) was added to the mixture under vigorously stirring and heated to 90 °C for 48 h. The mixture was then poured into distilled water (600 mL), extracted with chloroform, and dried with anhydrous magnesium sulfate. The solvent was removed under reduced pressure. The residue was dissolved in chloroform and then purified by silica-gel column chromatography with dichloromethane as the eluent. The product was obtained as a yellow powder after drying with 72% of yield (3.2 g). ^{1}H NMR ($CDCl_3$, TMS, δ): 9.79 (s, 1H), 6.87–7.65 (m, 7H), 3.90 (t, 2H), 1.79 (m, 2H), 1.48 (m, 2H), 0.95 (t, 3H).

Synthesis of 2,4,6-tris[2-(*N*-butyl-3-phenothiazine) carboxethenyl]-1,3,5-*s*-triazine (TP3T)

Under refluxing temperature, a solution of 2,4,6-trimethyl-1,3,5-*s*-triazine (0.135 g, 1.1 mmol) in methanol (5 mL) was added dropwise into a flask containing methanol (25 mL), tetrahydrofuran (THF, 25 mL), *N*-butyl-3-formyl-phenothiazine (0.934 g, 3.3 mmol), and potassium hydroxide for about 2 h. The reaction mixture was refluxed for a further 48 h. After cooling down to room temperature, the crude product was collected by filtration. Then it was purified by column chromatography on silica gel using toluene as the eluent. After evaporation to get rid of solvent under vacuum, a solid was obtained. Then we smashed it to powder and dried further in the oven. After that the reprecipitation with hexane/1,2-dichloroethane was repeated several times. After drying in vacuum at 80 °C, the product was obtained as a orange powder with 74% of yield (0.750 g) and characterized by elemental analysis, NMR, MS, and IR. Found: C, 74.31; H, 5.97; N, 9.01. Calcd for $C_{57}H_{54}N_6S_3$: C, 74.47; H, 5.92; N, 9.14. ^{1}H NMR ($CDCl_3$, δ): 8.11 (d, 3H), 7.44 (t, 6H), 7.21–6.86 (m, 18H), 3.86 (m, 6H), 1.78 (m, 6H), 1.44 (m, 6H), 0.95 (m, 9H). ^{13}C NMR ($CDCl_3$, δ): 171.08, 146.69, 144.33, 140.27, 129.94, 127.79, 127.50, 127.31, 126.74, 125.00, 124.22, 124.10, 122.80, 115.51, 115.24, 47.38, 28.95, 20.16, 13.81. ESI-MS (m/z) = 919.10; Calcd 919.27 (M^+). IR (KBr, cm^{-1}) = 2957, 2872, 1631, 1599, 1553, 1510, 1468, 1444, 1404, 1362, 742.

Device fabrication and characterization

To investigate the electroluminescent (EL) properties of the symmetric starburst system containing strong intramolecular charge-transfer, a single layer non-doped OLED was fabricated *via* solution process. TP3T was dissolved in 1,2-dichloroethane, filtered through a 0.22 μm filter and spin-coated on the indium tin oxide (ITO) substrate prepared according to our previous report.[23] As a comparison, tri(8-hydroxyquinoline) aluminium(III) (AlQ_3) was deposited to change the electron-transport by vacuum evaporation. An ultra thin layer of LiF and 100 nm of aluminium layer were evaporated in vacuum (5×10^{-6} torr) as the cathode, the area of which was defined as

active area of the devices (4 mm^2). The thickness of the evaporating layer was monitored with a quartz crystal microbalance. The devices were annealed at 70 °C for 30 min under vacuum to remove trace amount of solvent left by spin-coating. The device performances were measured with Keithley 2611 source meter and a spectrophotometer (Photo Research 650). All the measurements were carried out in ambient atmosphere at room temperature. The device structures of the non-doped OLEDs were as follows:

Device A: ITO/TP3T (70 nm) /LiF (0.5nm)/Al (120nm);

Device B: ITO/TP3T (40 nm) /AlQ_3 (30 nm)/LiF (0.5nm)/Al (120 nm).

Results and discussion

Physical properties

The starburst compound TP3T can be dissolved in common organic solvents, *e.g.*, THF, chloroform, dichloromethane, 1,2-dichloroethane, toluene, *etc.*, and shows a thermal-decomposition temperature (T_d) at 350 °C and a glass-transition temperature (T_g) at 63 °C. The UV-vis absorption and PL spectra of TP3T in THF solution and in thin film state are shown in Fig. 1. TP3T exhibits two absorption bands located at 310 nm and 428 nm, which are assigned to π–π* transition and intramolecular charge-transfer transition, respectively.[6] The absorption peak of TP3T is slightly red-shifted from 418 nm in cyclohexane to 428 nm in THF towards the solvents polarity increasing as previously reported,[24] which means the stronger ground state dipole of the molecule. From the onset absorption of film, the corresponding optical energy gap (E_g) of TP3T was calculated to be 1.98 eV. The absorption and emission peaks of TP3T film show red-shift compared to those obtained in the solution, which is caused by intermolecular interaction in the film. The PL spectrum peak of TP3T in THF solution and film is located at 568 nm and 586 nm, respectively. Its fluorescent quantum yield (Φ) is 0.42 (measured in toluene), which is much higher than that of the classical red laser-dye 4-(dicyanomethylene)-2-methyl-6-[4-(dimethylaminostyryl)-4*H*-pyran] (DCM, 0.08).[25] We attributed the high Φ value to the enhanced strength of intramolecular charge transfer, which can be proved by the rise of absorption band located around 450 nm compared with our previously reported compound.[15] As shown in Fig. 2, TP3T gives a fluorescence from 505–593 nm in solvents which is sensitive to solvent polarities (hexane < toluene < THF < chloroform), which can be explained by the typical Lippert-Mataga relationship as reported.[24] The solvatochromic behavior also indicates the existence of strong intramolecular charge-transfer character of TP3T, which was also found in a similar molecular structure.[8] As shown in the inset of Fig. 1, after the molecule is excited from ground state (D^{δ_0+}–A^{δ_0-}) to the excited state (D^{δ_1+}–A^{δ_1-})*, then it relaxes to a more stable low-lying charge transfer state (D^{δ_2+}–A^{δ_2-})*. The low-lying charge transfer state (D^{δ_2+}–A^{δ_2-})* is responsible for the long wavelength emission.[11] It is likely that the degree of charge transfer is such as $0 < \delta$ ($\delta_0 < \delta_1 < \delta_2$) < 1.

The highest occupied molecular orbital (HOMO) level of TP3T was estimated to be −5.04 eV. For the calibration, the redox potential of ferrocene/ferrocenium (Fc/Fc+), which is assumed an absolute energy level of −4.80 eV to vacuum,[26] was measured to be located at 0.51 V to the saturated calomel electrode (SCE). Therefore the HOMO energy can be calculated with the formula $E_{HOMO} = -(E_{ox} - E_{Fc/Fc+})$ eV + (−4.8) eV, in which E_{ox} is the oxidation potential of TP3T obtained by CV measurement with Pt disk as the working electrode, Pt wire the counter electrode, and a saturated calomel electrode (SCE) as the reference electrode in CH_2Cl_2 solution containing 0.1 M of tetrabutylammonium perchlorate as the supporting electrolyte. The lowest unoccupied molecular orbital (LUMO) level of TP3T could be calculated as −3.06 eV from the HOMO level and E_g.

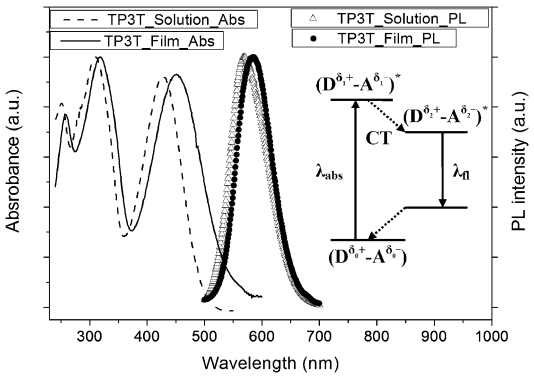

Fig. 1 Normalized UV-vis absorption (left) and PL (right) of TP3T in THF and film. Inset: proposed energy level diagram of the photophysical processes of TP3T.

Device performances

For single layer device A, which using TP3T as the single combination layer of charge transporting and emitter, its current density and luminance-voltage characteristics are shown in Fig. 3 and 4. The device has a low turn-on voltage of 2.5 V. The low driving voltage can be attribute to that the HOMO level of TP3T is close to the work function energy level of ITO as shown in the inset of Fig. 3, and its bipolar structure could also facilitate both hole and electron transport. The pristine device A achieved a maximum luminance of 1289 cd m^{-2} at 7.0 V.

To change the electron transport in device A, a layer of conventional electron transporting material (AlQ_3) was added (device B), in which TP3T acted as combinational hole

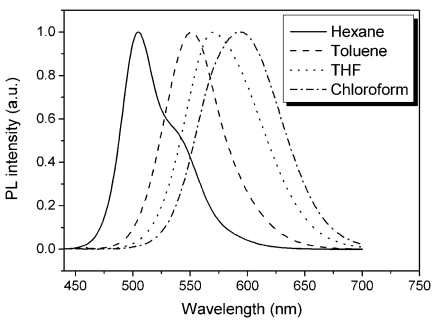

Fig. 2 Normalized PL spectra of TP3T in solvents with different polarity.

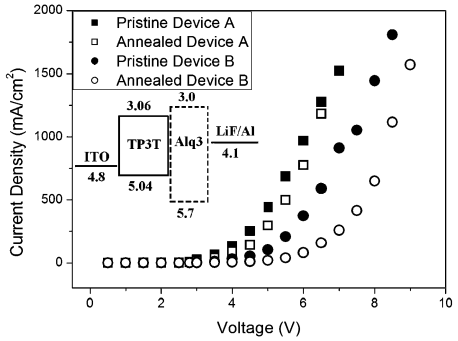

Fig. 3 Current density-voltage characteristics of single layer device A and double layer device B. Inset: energy level diagram of the devices.

transporting and emitting layer and AlQ_3 acted as electron transporting layer. However, the current density of device B is lower than that of device A, and the turn-on voltage of device B is 2.7 V, also higher than the single layer one. These might be due to that the higher lying LUMO level of AlQ_3 than TP3T make it harder for electron injection (inset of Fig. 3). In addition, the inserting of AlQ_3 layer may also induce a lower current density because more holes in the device B should be blocked due to the lower lying HOMO level of AlQ_3. However, less exciton quenching induced by the inserting of AlQ_3 layer between the metal cathode and the emitter layer may result in a higher efficiency. Actually as shown in Fig. 4, the pristine device B achieved a luminance of 4136 cd m^{-2}, higher than that of the pristine device A.

After annealing, the current density is lower and the performance of the device A is greatly improved with a maximum luminance of 2935 cd m^{-2} at an operating voltage of 7.0 V. This might result from the suppress of the defects and improvement of the interface contact between electrode and organic layer through annealing.[20] In addition, trace amount of solvent left in the organic layer *via* solution process could be removed by annealing treatment, which might improve the performance of the annealed device.

As a comparison, the double layer device B was also annealed at the same condition as the single layer device A. Unlike the single layer device A, although the current density and the luminance are lower after annealing, there was not much (80%) enhancement after annealing for the current effciency (CE) of device B, compared with 2.6 times more enhancement for the single layer device A (Fig. 5). Even the

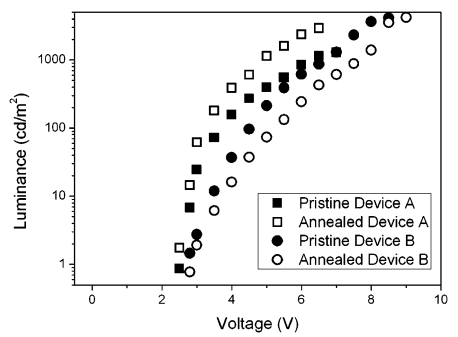

Fig. 4 Luminance-voltage characteristics of single layer device A and double layer device B.

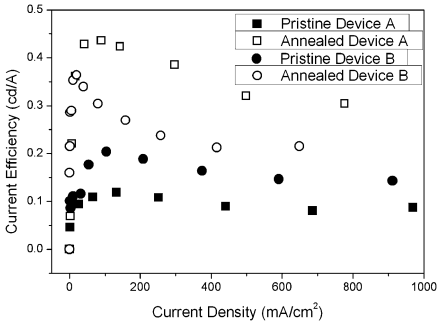

Fig. 5 Current efficiency-current density characteristics of single layer device A and double layer device B.

CE of device B after annealing is lower than that of the annealed device A. This might be interpreted that only the interface contact between anode and organic layer was improved in device B, but in single layer device A both interfaces contact between anode and cathode with the organic layer were improved. Furthermore, the bipolar characteristic of the starburst molecule, which endows it with balanced charge transport, may also result in a higher efficiency than that of the double layer device B after annealing. All the device performances are listed in Table 1.

The single layer device A exhibited a stable orange-red emission centered at 604 nm, the EL spectra only showed slightly blue-shift with the increasing of voltage, the shape of which was also unchangeable with CIE coordinates (0.59, 0.41) (Fig. 6). These indicate that TP3T has a stable emission property which might be due to the containing of phenothiazine moieties as our previous observation.[20,27] In addition, the small polarity of TP3T caused by symmetric conformation may also contributes to the EL spectra stability.[12]

Conclusions

In summary, we have synthesized a symmetric star-shaped orange-red emitter with a D-π-A structure. Because of the strong intramolecular charge transfer, it shows orange-red emission with high fluorescence quantum yield. Thanks to the smaller dipole moment for the molecule resulted from its symmetric starburst conformation and longer alkyl group, the starburst molecule could avoid severe concentration quenching in the solid state. Furthermore, the materials can be easily dissolved in common solvent, affording it possible for solution process. Owing to its bipolar structure, both hole and electron transport could be facilitated. Single layer non-doped orange-red OLED *via* solution process with a low turn-on voltage of

Table 1 Performance of single layer device A and double layer device B

Device		V_{on}	L_{max}/cd m^{-2}	CE_{max}/cd A^{-1}	CIE (x, y)
A	Pristine	2.5	1289	0.12	(0.59, 0.41)
	Annealed	2.5	2935	0.44	(0.59, 0.41)
B	Pristine	2.7	4136	0.20	(0.59, 0.41)
	Annealed	2.7	4217	0.36	(0.59, 0.41)

V_{on} is the turn-on voltage, L_{max} is the maximum luminance, CE_{max} is the maximum current efficiency.

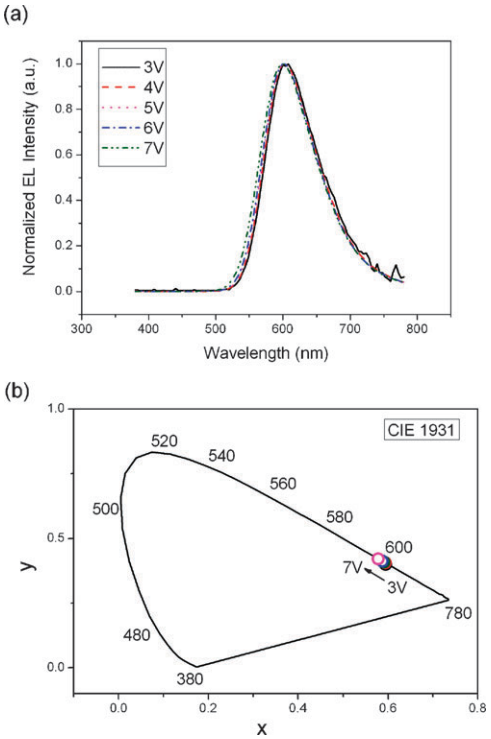

Fig. 6 Normalized EL spectra (a) and CIE coordinates (b) of the single layer device A at different driving voltages.

2.5 V, a maximum luminance of 2935 cd m^{-2} was achieved. The starburst molecule shows a stable orange-red emission with CIE coordinates (0.59, 0.41) under different driving voltages. These results may give some new suggestions for the molecular design of red emitters.

Acknowledgements

This work was financially supported by the National Natural Science Foundation of China under grant Nos. 60677002, 10674011, 10934001, 60907015, and 10821062, and the National Basic Research Program of China under grant Nos. 2007CB307000 and 2009CB930504.

Notes and references

1 C. W. Tang and S. A. VanSlyke, *Appl. Phys. Lett*., 1987, **51**, 913.
2 C. W. Tang, S. A. VanSlyke and C. H. Chen, *J. Appl. Phys*., 1989, **65**, 3610.
3 A. Tang, F. Teng, S. Xiong and Y. Hou, *Appl. Surf. Sci*., 2008, **254**, 2043.
4 H.-C. Yeh, S.-J. Yeh and C.-T. Chen, *Chem. Commun*., 2003, 2632.
5 Y. Zhou, Q. He, Y. Yang, H. Zhong, C. He, G. Sang, W. Liu, C. Yang, F. Bai and Y. Li, *Adv. Funct. Mater*., 2008, **18**, 3299.
6 S. Chen, X. Xu, Y. Liu, G. Yu, X. Sun, W. Qiu, Y. Ma and D. Zhu, *Adv. Funct. Mater*., 2005, **15**, 1541.
7 W.-C. Wu, H.-C. Yeh, L.-H. Chan and C.-T. Chen, *Adv. Mater*., 2002, **14**, 1072.
8 K. R. J. Thomas, J. T. Lin, M. Velusamy, Y.-T. Tao and C.-H. Chuen, *Adv. Funct. Mater*., 2004, **14**, 83.
9 H. Li, Y. Hu, Y. Zhang, D. Ma, L. Wang, X. Jing and F. Wang, *J. Polym. Sci., Part A: Polym. Chem*., 2004, **42**, 3947.
10 C.-T. Chen, *Chem. Mater*., 2004, **16**, 4389.
11 L. Xiao, H. Shimotani, N. Dragoe, A. Sugita, K. Saigo, Y. Iwasa, T. Kobayashi and K. Kitazawa, *Chem. Phys. Lett*., 2003, **368**, 738.
12 M. Xu, Z. Chen, L. Xiao and Q. Gong, *J. Phys. D: Appl. Phys*., 2009, **42**, 055116.
13 O. A. Matthews, A. N. Shipway and F. F. Stoddart, *Prog. Polym. Sci*., 1998, **23**, 1.
14 H. Frey, C. Lach and K. Lorenz, *Adv. Mater*., 1998, **10**, 279.
15 B. Qu, Z. Chen, F. Xu, H. Cao, Z. Lan, Z. Wang and Q. Gong, *Org. Electron*., 2007, **8**, 529.
16 H. Spreitzer and J. Daub, *Chem.–Eur. J*., 1996, **2**, 1150.
17 M.-J. Park, J. Lee, J.-H. Park, S. K. Lee, J.-I. Lee, H.-Y. Chu, D.-H. Hwang and H.-K. Shim, *Macromolecules*, 2008, **41**, 3063.
18 M.-S. Yuan, Q. Fang, Z.-Q. Liu, J.-P. Guo, H.-Y. Chen, W.-T. Yu, G. Xue and D.-S. Liu, *J. Org. Chem*., 2006, **71**, 7858.
19 X. Liu, H. Xia, Y. Ma and Y. Mu, *Thin Solid Films*, 2009, **517**, 5584.
20 Y. Liu, H. Cao, J. Li, Z. Chen, S. Cao, L. Xiao, S. Xu and Q. Gong, *J. Polym. Sci., Part A: Polym. Chem*., 2007, **45**, 4867.
21 C. S. Fred and P. J. Gracea, *J. Org. Chem*., 1961, **26**, 2778.
22 H. K. Jung, C. L. Lee and J. K. Lee, *Thin Solid Films*, 2001, **401**, 111.
23 J. Luo, L. Xiao, Z. Chen and Q. Gong, *Appl. Phys. Lett*., 2008, **93**, 133301.
24 W. Feng, S. Kong, L. Xiao, K. Meng, S. Wang and Q. Gong, *Chin. Phys. Lett*., 2009, **26**, 127801.
25 C.-L. Chiang, M.-F. Wu, D.-C. Dai, Y.-S. Wen and J.-K. Wang, *Adv. Funct. Mater*., 2005, **15**, 231.
26 J. Pommerehne, H. Vestweber, W. Guss, R. F. Mahrt, H. Bassler, M. Porsch and J. Daub, *Adv. Mater*., 1995, **7**, 551.
27 Y. Liu, H. Cao, J. Li, Z. Chen, L. Xiao, Q. Gong and S. Shao, *Polym. Adv. Technol*., 2008, **19**, 1839.

